PERGAMON

Phytochemistry 55 (2000) 327–336

PHYTOCHEMISTRY

www.elsevier.com/locate/phytochem

Anthocyanic vacuolar inclusions — their nature and significance in flower colouration

Kenneth R. Markham [a,*], Kevin S. Gould [b], Chris S. Winefield [c], Kevin A. Mitchell [a], Stephen J. Bloor [a], Murray R. Boase [c]

[a] *NZ Institute for Industrial Research and Development, PO Box 31310, Lower Hutt, New Zealand*
[b] *School of Biological Sciences, University of Auckland, Private Bag 92019, Auckland, New Zealand*
[c] *Crop and Food Research Ltd., Private Bag 11600, Palmerston North, New Zealand*

Received 16 September 1999; received in revised form 26 April 2000

Abstract

The petals of a number of flowers are shown to contain similar intensely coloured intravacuolar bodies referred to herein as anthocyanic vacuolar inclusions (AVIs). The AVIs in a blue-grey carnation and in purple lisianthus have been studied in detail. AVIs occur predominantly in the adaxial epidermal cells and their presence is shown to have a major influence on flower colour by enhancing both intensity and blueness. The latter effect is especially dramatic in the carnation where the normally pink pelargonidin pigments produce a blue-grey colouration. In lisianthus, the presence of large AVIs produces marked colour intensification in the inner zone of the petal by concentrating anthocyanins above levels that would be possible in vacuolar solution. Electron microscopy studies on lisianthus epidermal tissue failed to detect a membrane boundary in AVI bodies. AVIs isolated from lisianthus cells are shown to have a protein matrix. Bound to this matrix are four cyanidin and delphinidin acylated 3,5-diglycosides (three, new to lisianthus), which are relatively minor anthocyanins in whole petal extracts where acylated delphinidin triglycosides predominate. Flavonol glycosides were not bound. A high level of anthocyanin structural specificity in this association is thus implied. The specificity and effectiveness of this anthocyanin "trapping" is confirmed by the presence in the surrounding vacuolar solution of only delphinidin triglycosides, accompanied by the full range of flavonol glycosides. "Trapped" anthocyanins are shown to differ from solution anthocyanins only in that they lack a terminal rhamnose on the 3-linked galactose. The results of this study define for the first time the substantial effect AVIs have on flower colour, and provide insights into their nature and their specificity as vacuolar anthocyanin traps.

Keywords: *Eustoma grandiflorum*; *Dianthus caryophyllus*; Petal colour; Anthocyanic vacuolar inclusions; Anthocyanin; Protein; Trap

1. Introduction

Anthocyanin pigments impart colour to the petals of many plant species. In most plants these pigments are normally found dissolved uniformly in the vacuolar solution of epidermal cells. However, in certain species, the anthocyanins are localised in discrete regions of the cell vacuole. Such pigmented bodies have been described as "blue spherules" in epidermal rose petal cells (Yasuda, 1974), "intravacuolar spherical bodies" in *Polygonum cuspidatum* seedlings (Kubo et al., 1995), "ball-like structures" and "crystals" in stock, *Matthiola incana*, petals (Hemleben, 1981), "blue crystals" in larkspur, *Consolida ambigua*, petals (Asen et al., 1975) and red "crystals" in mung bean hypocotyl (Nozzolillo and Ishikura, 1988). Little has been documented about the structure, chemical nature, or functional significance of these inclusions in petal cells. However, other structures that occur in the leaves of various Brassicaceae (Small and Pecket, 1982; Nozzolillo et al., 1995), in the tubers of the sweet potato, *Ipomoea batatas* (Nozue et al., 1997), and in grapes (Cormier and Do, 1993) have received some attention. Early reports (Pecket and Small, 1980) described these spherical bodies as "anthocyanoplasts", membrane-bound organelles that provide intense colouration in the vacuoles of mature plant cells. More recent reports however indicate that these globular inclusions may be protein matrices

* Corresponding author. Tel.: +64-4-569-0000; fax: +64-4-569-0055.
E-mail address: k.markham@irl.cri.nz (K.R. Markham).

0031-9422/00/$ - see front matter
PII: S0031-9422(00)00246-6

(Nozue et al., 1995, 1997), and that they possess neither a membrane boundary nor an internal structure (Nozzolillo, 1994, Cormier, 1997; Nozue et al., 1997).

Although reference is made in the literature to pre-1940 observations of "anthocyanoplasts" in flower petals (Pecket and Small, 1980), their relationship to the more recently studied leaf anthocyanoplasts is unclear, and the significance of these bodies to flower colour seems not to have been recognised. The present paper details our own studies on the vacuolar inclusions in the petals of carnation (*Dianthus caryophyllus*) and lisianthus (*Eustoma grandiflorum*). These inclusions are referred to herein as "anthocyanic vacuolar inclusions" (AVIs). The evidence presented defines these as membrane-less, proteinaceous matrices with a high specific affinity for certain anthocyanin-3,5-diglycosides. Their presence is shown to have a profound effect on both petal colour and intensity. Such information is of potential significance to plant breeders and molecular biologists interested in the production of novel coloured flowers.

2. Results and discussion

In the course of the present study a wide range of flowers has been examined for the presence of AVIs. AVIs have been observed in only a few of these, namely cultivars of *Salvia*, *Antirrhinum*, *Dianthus*, *Lisianthius*, *Eustoma* (lisianthus), *Sinningia* and *Delphinium* flowers. Their presence commonly has an observable effect on flower colour. This may be in the form of a marked intensification of colour as seen in *Eustoma grandiflorum* (lisianthus), or a shift to bluer colour as in *Dianthus caryophyllus* (carnation). These two species were chosen as models in the present study to investigate further, the nature of AVIs and their effect on flower colour.

2.1. Purple lisianthus (*Eustoma grandiflorum*) and the nature of AVIs

One of the purple lisianthus cultivars (# 54) used for this study has been the subject of several previous pigment-related investigations (Markham and Ofman, 1993; Markham, 1996; Schwinn et al., 1997; Deroles et al., 1998) and the other, Wakamurasaki, possesses an identical pigment profile. A feature of the colour in these flowers is the intense blackish-purple zone at the base of the petal (inner petal) and a larger, lighter purple "outer" petal area (Fig. 1a). Microscopic examination of adaxial epidermal peels from these zones, and from intermediate zones, revealed that cells in the inner petal contain one and occasionally more, large and intensely coloured AVIs of irregular shape (Fig. 1b). The frequency and size of these AVIs diminish markedly in the intermediate and outer zones. In contrast, AVIs in the outer zone are thread-like or granular in shape (Fig. 1c) and many cells lack AVIs completely. Examination of transverse sections revealed that pigmentation (including AVIs) in all zones is found predominantly in the adaxial epidermal layer of cells with pigmented cells appearing only occasionally in the abaxial epidermis (Fig. 1d).

The presence of AVIs in purple lisianthus has a significant effect on petal colour intensity and hue. Absorptance/reflectance spectra of inner and outer petal zones measured with an integrating sphere, indicated a distinct bluing of colour in the AVI-rich inner petal. This bluing was evidenced by enhanced absorptance in the longer wavelength bands at 625 nm. Thus, in the outer petal, absorptance at 625 nm was 79% of the intensity of the 545 and 575 nm peaks whilst in the inner petal it was 95%.

The lisianthus AVIs could be removed from cell vacuoles using narrow glass micropipettes. They remained intact, and adhered firmly to the glass indicating that they are structural rather than localised concentrations of dissolved anthocyanins. Since it has been proposed that similar (spherical) structures in red cabbage foliage ("anthocyanoplasts") are functional membrane-bound organelles (Small and Pecket, 1982), an examination of structure using electron microscopy was undertaken. Electron micrographs of transverse sections through lisianthus petals (data not shown) confirmed the light microscopy observation that the AVIs are irregular in shape and lack a membrane boundary. They appear therefore not to be organelles.

Vacuoles that contained AVIs could be distinguished from other vacuoles on the basis of their reaction to Ponceau 2R, a general protein stain (Harris, 1983). The AVIs stained red with Ponceau 2R under bright field microscopy and fluoresced red with UV under epi-fluorescence, indicating the presence of protein. Colourless vacuoles and vacuolar sap surrounding the AVIs did not show these staining reactions. When transverse sections through petals were infused with HOAc on a microscope slide, some red pigment was liberated. The likely composition of these AVIs is, therefore, that of a protein matrix to which anthocyanins are non-covalently bound.

In order to gain further information about the AVIs present in the inner petal of lisianthus flowers, AVI-containing protoplasts were isolated from this tissue by enzymic dissolution of the cell wall followed by density gradient centrifugation. Sonication released the contents from these protoplasts and AVIs were collected by a second round of density gradient centrifugation. Microscopy confirmed their irregular, jelly-like form (Fig. 1e). The AVIs were found to be insoluble in most aqueous buffers and were not solubilised with common detergents such as SDS, Triton X-100 or Nonidet P40. They were also only partially soluble in concentrated denaturing solutions such as 6 M urea and 6 M guanidine hydrochloride. Complete solubilisation in fact was

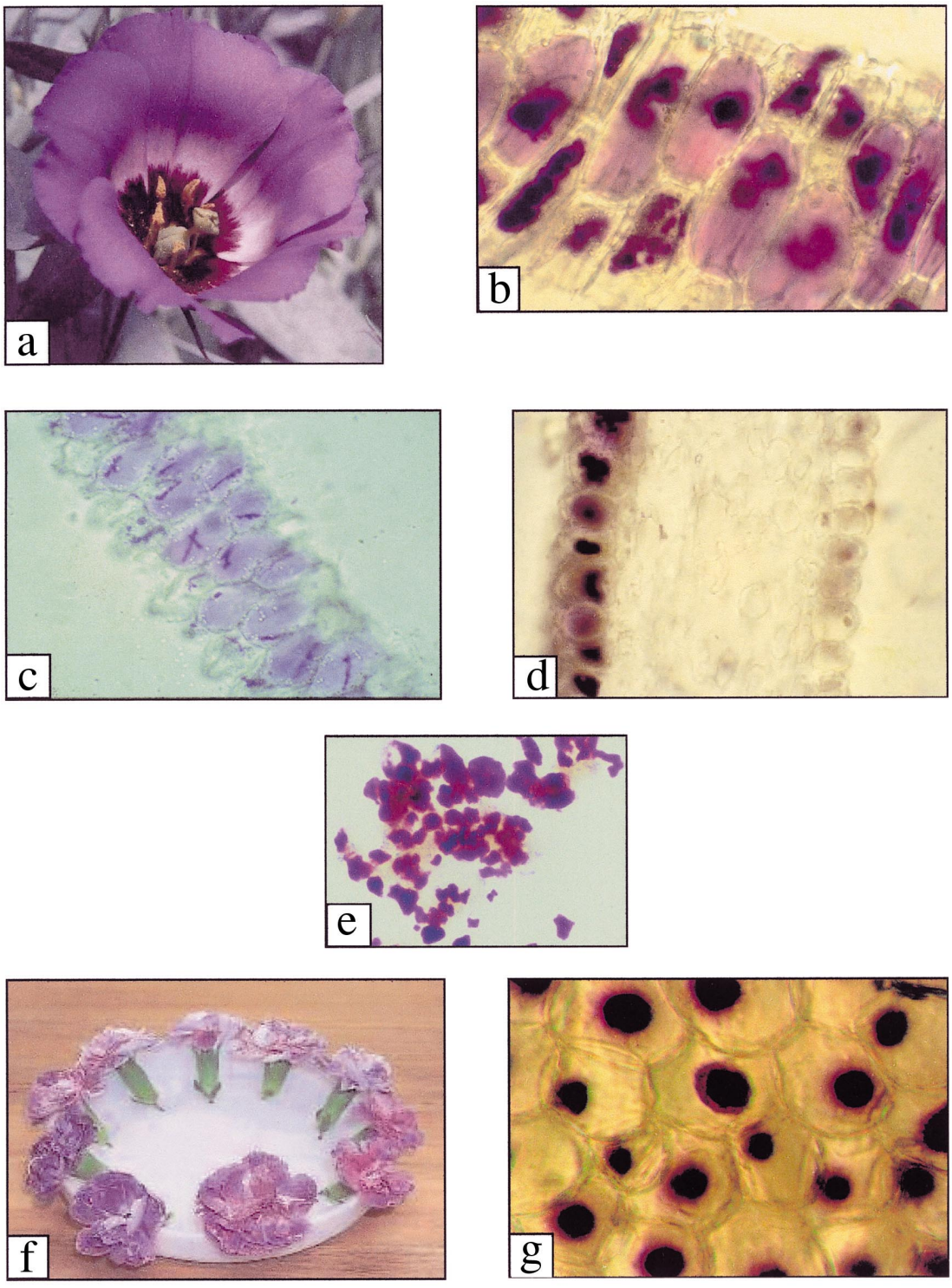

Fig. 1. (a) Purple flower of *Eustoma grandiflorum* (lisianthus), line 54; (b) AVIs in an oblique hand-section of the adaxial epidermal peel of the deep purple inner petal region of *Eustoma grandiflorum*; (c) AVIs in an oblique hand-section of the adaxial epidermal peel of the light purple outer petal region of *Eustoma grandiflorum*; (d) Transverse section through the inner petal region of *Eustoma grandiflorum* cv Wakamurasaki; (e) AVIs isolated from *Eustoma grandiflorum*, line 54, inner petal region; (f) Blue-grey and pink flowers of *Dianthus caryophyllus*; (g) AVIs in an adaxial epidermal peel of *Dianthus caryophyllus*. Note: degree of magnification varies.

only achieved with high concentrations of both denaturant and reductant, i.e. in a solution containing 9.8M urea, 2% Triton X-100, 100 mM Tris–Cl and 100 mM dithiothreitol. Electrophoretic fractionation of the solubilised material using 2D-IEF revealed three major protein species which were detected with both Coomassie and silver staining (Fig. 2). These proteins were found to have approximate molecular weights of 50,000, 35,000 and 34,000 Daltons and pIs (pHs at net zero charge) in the range 4–5. Further characterisation of the protein complement of the AVIs is currently in progress and will form the basis of a future communication.

The anthocyanin pigment components of lisianthus AVIs were extracted from isolated AVIs with MeOH/HOAc, analysed by HPLC and compared with pigments obtained from whole petal, outer petal and inner petal extracts. Two features of the AVI pigment profile were immediately evident. Firstly, the flavonol copigments which are present in whole petal extracts at ca. 8× the level of the anthocyanins (Markham and Ofman, 1993), are not associated with the AVIs. Secondly, only four anthocyanins out of the nine evident in HPLCs of whole petal extracts are bound to the AVIs (Fig. 3). These four anthocyanins are the relatively minor components represented by peaks 2, 3, 6 and 7 in the whole petal extract (Fig. 3). They are virtually absent in the outer petal, but are significant components of the much smaller inner petal.

The structures of the four anthocyanins bound to AVIs were established by HPLC, TLC, absorption spectroscopy and mass spectrometry. Previous work (Asen et al., 1986; Markham and Ofman, 1993; Markham, 1996) has established that the three major pigments in purple lisianthus cultivars are delphinidin-3-*O*-β-D-(6-*O*-α-L-rhamnopyranosylgalactopyranoside)-5-*O*-β-D-(6-*E*-*p*-coumaroylglucopyranoside) (**4**), its *Z*-isomer (**1**) and its ferulylated equivalent (**5**). These compounds are represented by the larger HPLC peaks, 4, 1 and 5 respectively (Fig. 3), as indicated from previously published data (Schwinn et al., 1997), relative peak intensities and on-line measured spectra. Of the minor components, only two, delphinidin- and cyanidin-3-galactoside-5-(6-*p*-coumaroyl-glucoside) (**2** and **6**), have been recognised previously (Markham and Ofman, 1993). Peak 2 is the only unassigned peak for which data are consistent with a mono-*p*-coumaroylated (λ_{max} 279, 300, 315 sh), 3,5,-glycosylated delphinidin (λ_{max} 527 nm with no significant shoulder at 440 nm) formulation. The other minor delphinidin based pigment (peak 3) has absorption in the UV (λ_{max} 290, 327 nm), consistent with the equivalent mono-ferulylated derivative. The previously reported acylated cyanidin diglycoside (**6**) is represented by one of the four later peaks (peaks 6, 7, 8 and 9) which give 3,5-glycosylated cyanidin-type spectra (λ_{max} 518 nm with no significant shoulder at 440 nm). These four components appear to be a set of four matching the delphinidin glycosides. Two peaks, 6 and 8, are defined by their UV absorption as mono-*p*-coumaroyl derivatives and two, peaks 7 and 9, as mono-ferulyl derivatives. By analogy with the delphinidin series, cyanidin-3-galactoside-5-(6-*p*-coumaroylglucoside) (**6**) is represented by the peak 6 and its ferulyl equivalent by

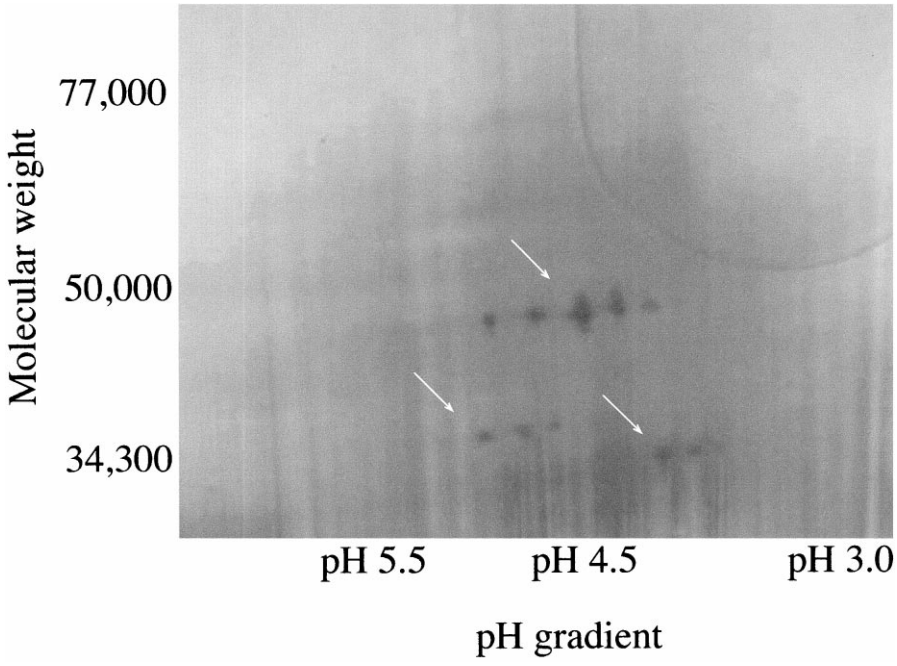

Fig. 2. Silver stained two-dimensional isoelectric focusing electropherogram of solubilised isolated AVI complexes. The major protein species are indicated with an arrow.

peak 7. The two cyanidin triglycosides likewise are represented by peaks 8 and 9. On the basis of the above assignments, the four AVI-bound anthocyanins are defined as delphinidin-3-galactoside-5-(6-*p*-coumaroylglucoside) (**2**) and its ferulyl equivalent (**3**), and cyanidin-3-galactoside-5-(6-*p*-coumaroylglucoside) (**6**) and its ferulyl equivalent (**7**). The last three of these pigments have not been recognized in lisianthus flowers previously. Confirmation of two of these structures was obtained from electrospray-MS of an extract of the isolated AVIs. Although the presence of proteinaceous material added complexity to the MS, a negative ion scan revealed clear major ions at *m/e* 787.6 and 803.6 which represent the molecular ions of monoferulylated cyanidin- and delphinidin-3-galactoside-5-glucoside pigments. The identity of a third, delphinidin-3-galactoside-5-(6-*p*-coumaroylglucoside), was confirmed by electrospray-MS of a sample purified from a whole petal extract. This produced one major ion at *m/e* 773.1 (+Ve ion mode) which is consistent with the proposed formulation. The diglycosidic nature of these AVI-bound anthocyanins is also supported by their consistently lower TLC mobility in HCl:HCO_2H:H_2O (1:1:2) relative to their triglycosidic analogues. AVIs isolated from the other purple lisianthus cultivar studied, Wakamurasaki, which has a pigment profile identical to cv #54, yielded the same selection of anthocyanins (Table 1).

The association between AVIs and anthocyanins in these examples thus appears to be highly selective, a view that finds further support in the analysis of the vacuolar solution surrounding the inclusions. Vacuolar solutions from 800 inner petal epidermal cells were individually removed using fine glass micropipettes and analysed by applying the combined vacuolar contents in one injection onto an HPLC column. As expected, the flavonol glycoside profile was the same as that of the inner petal extract, but the anthocyanin profile contained only two peaks, 1 and 4/5. These represent delphinidin-3-(6-rhamnogalactoside)-5-(6-*Z*-*p*-coumaroylglucoside) (**1**)

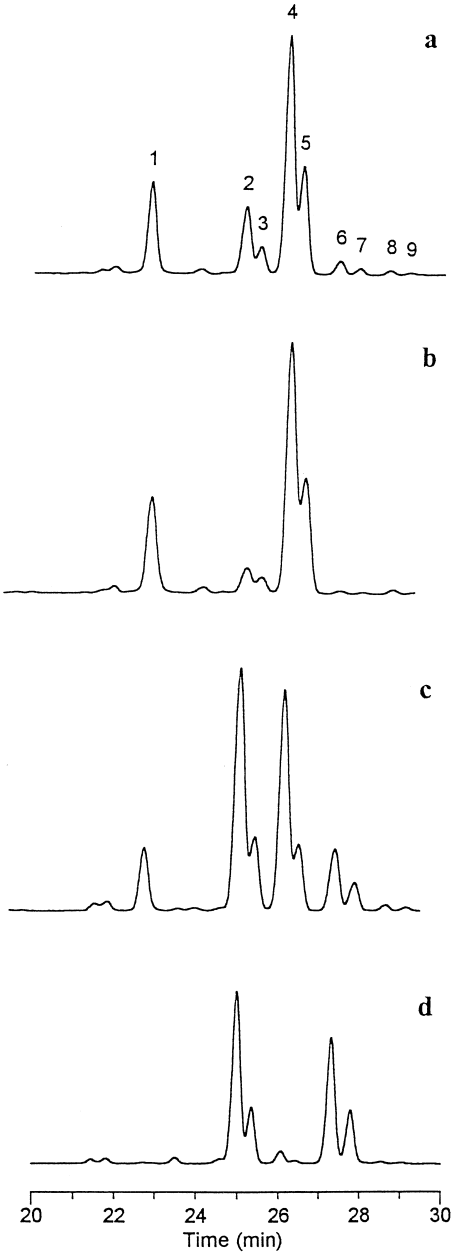

Fig. 3. HPLC profiles of anthocyanins present in extracts of (a) whole petal, (b) outer petal region, (c) inner petal region, and (d) AVIs, from *Eustoma grandiflorum*, line 54. Pigment structures: **1**, Delphinidin-3-*O*-β-[6-*O*-α-rhamnosylgalactoside]-5-*O*-β-[6-*O*-*Z*-*p*-coumaroylglucoside]; **2**, Delphinidin-3-*O*-β-galactoside-5-*O*-β-[6-*O*-*E*-*p*-coumaroylglucoside]; **3**, Delphinidin-3-*O*-β-galactoside-5-*O*-β-[6-*O*-*E*-ferulylglucoside]; **4**, Delphinidin-3-*O*-β-[6-*O*-α-rhamnosylgalactoside]-5-*O*-β-[6-*O*-*E*-*p*-coumaroylglucoside]; **5**, Delphinidin-3-*O*-β-[6-*O*-α-rhamnosylgalactoside]-5-*O*-β-[6-*O*-*E*-ferulylglucoside]; **6**, Cyanidin-3-*O*-β-galactoside-5-*O*-β-[6-*O*-*E*-*p*-coumaroylglucoside]; **7**, Cyanidin-3-*O*-β-galactoside-5-*O*-β-[6-*O*-*E*-ferulylglucoside]; **8**, Cyanidin-3-*O*-β-[6-*O*-α-rhamnosylgalactoside]-5-*O*-β-[6-*O*-*E*-*p*-coumaroylglucoside]; **9**, Cyanidin-3-*O*-β-[6-*O*-α-rhamnosylgalactoside]-5-*O*-β-[6-*O*-*E*-ferulylglucoside].

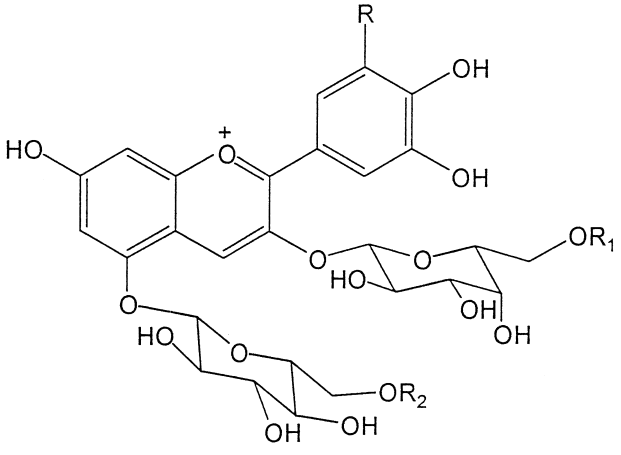

Structure. Delphinidin glycosides (R = OH): **1** R_1 = α-L-rhamnosyl; R_2 = *Z*-*p*-coumaroyl; **2** R_1 = H; R_2 = *E*-*p*-coumaroyl; **3** R_1 = H; R_2 = *E*-ferulyl; **4** R_1 = α-L-rhamnosyl; R_2 = *E*-*p*-coumaroyl; **5** R_1 = α-L-rhamnosyl; R_2 = *E*-ferulyl; Cyanidin glycosides (R = H): **6** R_1 = H; R_2 = *E*-*p*-coumaroyl; **7** R_1 = H; R_2 = *E*-ferulyl; **8** R_1 = α-L-rhamnosyl; R_2 = *E*-*p*-coumaroyl; **9** R_1 = α-L-rhamnosyl; R_2 = *E*-ferulyl.

Table 1
Major anthocyanins as percentages of total anthocyanins in various petal zones and in AVIs of purple lisianthus[a]

Petal zone	Delphinidin-5-*O*-(6-*O*-acylglucoside)[b]		Cyanidin-5-*O*-(6-*O*-acylglucoside)[b]	
	3-*O*-galactoside (2+3)	3-*O*-rhamnogalactoside (1+4+5)	3-*O*-galactoside (6+7)	3-*O*-rhamnogalactoside (8+9)
Cultivar # 54				
Whole petal	16.8	75.2	3.8	1.4
Outer zone	8.4	87.9	<1	<1
Inner zone	40.0	44.2	11.9	1.5
AVIs	49.7	4.9	40.4	1.1
Wakamurasaki				
AVIs	53.8	4.6	37.9	<1

[a] Figures based on HPLC peak integrals measured at 530 nm.
[b] Combined *p*-coumaroyl and ferulyl derivatives, both ***E*** and ***Z*** forms.

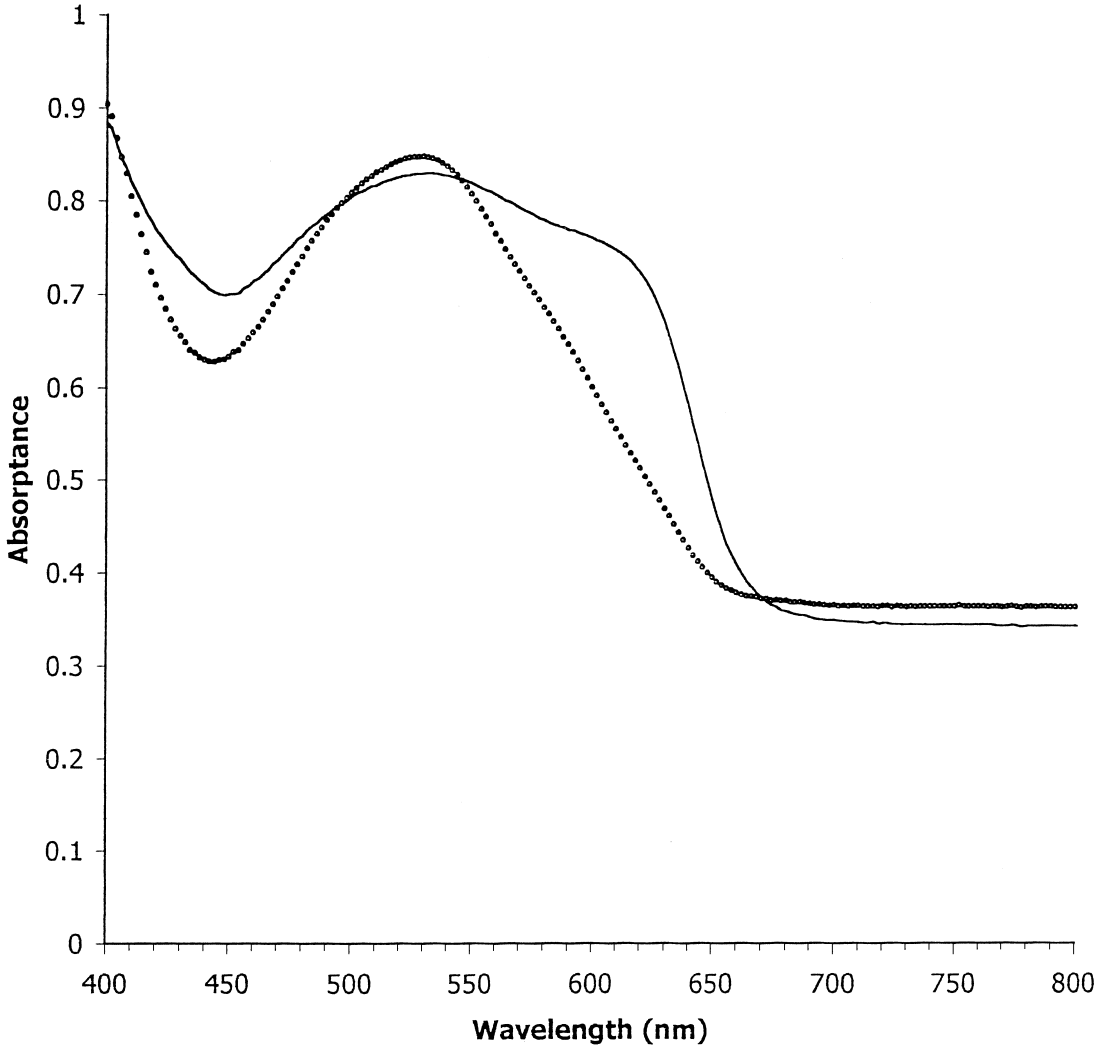

Fig. 4. Absorptance spectra of pink (····) and blue-grey (—) petals of *Dianthus caryophyllus* as measured using an Li 1800-12 integrating sphere.

and delphinidin-3-(6-rhamnogalactoside)-5-(6-*E*-*p*-coumaroyl/ferulyl-glucoside) (**4**/**5**), the major anthocyanins present in inner petal extracts but absent from the inclusions (Fig. 3). The inclusion-bound anthocyanins were not evident, thus confirming the strong level of structural selectivity involved in this protein-anthocyanin association. The possible involvement of metal ions in this association was excluded via a study of AVI

metal composition using ICP-MS. This demonstrated that none of the sixty-four quantified metals are found at higher levels in the AVIs than in the whole petal extract, and thus are not concentrated in AVIs.

2.2. Blue-grey carnation (*Dianthus caryophyllus*)

A blue-grey carnation was chosen as a second flower type for this study as it provides an excellent example of the bluing effect of AVIs. Blue-grey is a highly unusual colour for carnation, and flowers of this colour together with pink and mottled (Fig. 1f) were grown from a tissue culture of a blue-grey flower discovered in a commercial mix. Microscopic examination of adaxial epidermal peels (and transverse sections) revealed the presence of a single deep red AVI in each cell vacuole of the blue-grey tissue, with little or no visible pigmentation in the rest of the vacuole (Fig. 1g). In contrast, epidermal cells of pink petals, or of pink portions of the mottled petals, lacked AVIs but contained vacuoles that were homogeneously pigmented pink. Transverse sections of both tissue types revealed under microscopy that the AVI containing and pink pigmented vacuoles are confined predominantly to the adaxial epidermal cells. The difference in colour between the two basic petal types was quantified by measuring absorptance/reflectance spectra of whole petals using an integrating sphere connected to a spectroradiometer, which gave absorptance $\lambda_{(max)}$ values of 525 nm for the pink petals and 525, 610 nm for the blue-grey (Fig. 4). Absorption spectra of epidermal peels revealed a similar difference with the pink tissue exhibiting a peak at 528 nm with a small shoulder at 575 nm and the blue-grey, broadened peaks at 550 and 610 nm.

HPLC analyses of the anthocyanin pigments in both the blue-grey and pink tissue produced the same profile of one major (RT 12.54 min) and one minor (RT 14.64 min) peak. The absorption spectra of these peaks (λ_{max} 501–503 nm) indicate that both are pelargonidin glycosides. An additional absorption peak at 426 nm in the spectrum of the minor compared with a lower intensity shoulder in the major suggests that these anthocyanins are 3-glycosylated and 3,5-glycosylated respectively (Harborne, 1967). In fact, they proved to be chromatographically and spectroscopically identical with authentic pelargonidin-3-glucoside and 3,5-diglucoside from *Pelargonium* (Mitchell et al., 1998). Pelargonidin glycosides have been reported in pink carnations previously (Gonnet and Hieu, 1992), but their occurrence as the only anthocyanin in a blue hued flower of any kind has not to our knowledge been reported previously.

Blue colouration in anthocyanic petals normally results from some combination of acylated anthocyanin (commonly delphinidin based), high vacuolar pH and inter- or intra-copigmentation (Brouillard and Dangles, 1994). In the present case it is difficult to account for the difference in colour between pink and blue-grey petals by any of these criteria. Both tissue types have pH levels of about 5.6 as measured from macerates, and both contain the same *non-acylated* anthocyanins and flavonols. The ratios of anthocyanins to flavonols, which could be an indicator of any copigmentation reaction, is 0.9 for the pink tissue and >8.5 for the blue-grey. Such ratios are not consistent with the existence of a more effective inter-molecular copigmentation interaction in the blue-grey tissue. The absolute level of anthocyanins in the blue-grey tissue as measured spectrophotometrically, is four times that in the pink. This much higher level of anthocyanins in the blue-grey petals is associated almost entirely with the AVIs as little colour is seen in the surrounding vacuolar solution. The presence of AVIs thus appears to be the predominant factor that accounts for the colour differential observed.

3. Conclusion

The results above describe the nature of AVIs in lisianthus petals and highlight the significant influence that they can have on flower petal colour, strikingly exemplified in carnation. Surprisingly this is a field that has received scant comment in the literature to date, yet it is of potential value to plant breeders and molecular biologists interested in the production of novel coloured flowers.

The protein matrix of the lisianthus AVIs is of particular interest as it exhibits a high degree of specificity to anthocyanins, as distinct from other vacuolar phenolics, and to anthocyanin structure. Flavonol glycosides are not bound to this matrix, nor are the major acylated anthocyanidin triglycosides, which differ from the 'attached' anthocyanins only in that they contain one extra sugar. The 'attachment' of anthocyanins to the matrix protein is likely to be via H-bonding (since they are liberated with acetic acid containing solvents) to a sterically restricted site (in view of the apparent molecular size limitation). At the pH of the vacuole, however, the bonding is strong and the protein acts as an effective vacuolar trap for the acylated anthocyanidin *diglycosides* (which are not found in the surrounding vacuolar solution). By concentrating anthocyanins above levels that would be possible as a solution within the volume of the cell vacuole, this trapping effect would account for the observed colour intensification brought about by AVIs. The bluing effect could be the result of a concomitant equilibrium shift favouring the quinonoidal base forms of the anthocyanin due either to the bonding, or to self association (Hoshino and Goto, 1990). Support for this is found in the absorptance spectrum of the AVI-rich inner petals in which the band at ca. 625 nm is enhanced. Absorption in the 580–625 nm region is attributed to the presence of anthocyanin quinonoidal bases in either neutral or ionized forms

(Hoshino and Goto, 1990; Lin et al., 1992; Brouillard and Dangles, 1994; Baranac et al., 1996).

A more detailed investigation of the AVI protein and the nature of its bonding with, and effects on, the associated anthocyanins, is currently underway and will form the subject of a subsequent communication.

4. Experimental

4.1. Plant material

The lisianthus lines used in this study were lines # 54 and Wakamurasaki (see Deroles et al., 1998 for further details). Fully open flowers were harvested and washed with distilled water to remove potential contaminants such as pollen grains. Various petal regions were excised with a razor blade for further study. Blue-grey carnation plants were generated from flower cuttings obtained from a commercial mix. Nodal segments from flowering stalks (pedicles) were surface sterilized in a 0.8% sodium hypochlorite solution containing a few drops of Tween 20. Explants were rinsed and placed on shoot development medium (SDM) comprising MS salts (Murashige and Skoog, 1962), LS vitamins (Linsmaier and Skoog, 1965), 1 mg/l 1-naphthaleneacetic acid (NAA), 1 mg/l 6-benzylaminopurine (BAP), 30 g/l sucrose and 7.5 g/l agar. Axillary shoots emerged from buds and were transferred after several weeks to rooting medium (RM) comprising MS salts, LS vitamins, 0.1 mg/l NAA, 30 g/l sucrose and 7.5 g/l agar. Shoots elongated in this medium and flowered, and were multiplied further by adventitious micropropagation in multiplication medium comprising MS salts, B5 vitamins (Gamborg et al., 1976), 0.5 mg/l indole-3-butyric acid (IBA), 0.3 mg/l BAP, 0.1 mg/l gibberellic acid (GA_3), 30 g/l sucrose and 7.5 g/l agar. Adventitious shoots were transferred to RM before transplantation to potting mix. All media were adjusted to pH 5.7 after agar addition and were autoclaved for 15 min at 121°C and 103 kPa. All tissue cultures were maintained at 22°C +/− 3°C.

4.2. Protoplast generation and isolation

Protoplasts were generated from macerated inner petal material as described by Morgan (1998). Material from 10 flowers was added to a protoplasting solution containing 1% cellulase Onozuka R-10 (Yakult Honsha Co., Higashi-Shinbashi, Minatoku, Tokyo) and 0.05% Pectolyase Y23. The mix was incubated overnight at room temperature and then filtered through a 50 μm stainless steel mesh, washed in 1/10 strength VKM macro salts (Binding and Nehls, 1977) plus 17.53 g/l NaCl (wash solution), and the protoplasts collected by centrifugation (100 × *g*, 5 min). The pelleted protoplasts were washed twice with wash solution.

4.3. AVI isolation

To enrich for protoplasts containing the AVIs, isolated protoplasts were subjected to centrifugation through a 4 step discontinuous Percoll (AMRAD-Pharmacia Biotech, Auckland, NZ) gradient (20%, 30%, 50%, 80% v/v, Percoll/wash solution). The gradient was formed by careful sequential addition of equal volumes of each gradient solution in descending order. Isolated protoplasts in wash solution were added to the top of the gradient and the gradient developed by centrifugation (300 × *g*, 5 min in a swing-out bucket rotor). Intensely pigmented protoplasts containing AVIs were collected from the 50%/80% boundary and washed twice with wash solution. The AVI-containing protoplasts were lysed using sonication and the product was carefully layered onto a second Percoll gradient which was developed as described above. Isolated AVIs pelleted at the bottom of the centrifuge tube and were washed twice with wash solution.

4.4. Optical properties of petals

The optical properties of 10 mm-diameter discs from the inner and outer regions of whole petals were determined using a Li 1800-12 integrating sphere connected to a Li 1800 spectroradiometer via a fibre optic cable (LiCor, Lincoln, Nebraska). Reflectance and transmittance were determined at 2 nm intervals over the 400–1100 nm waveband, referenced to a barium sulphate standard. Absorptance was calculated as 1-transmittance-reflectance. Adaxial epidermal peels for absorption spectroscopy were obtained by firmly applying transparent adhesive tape to both adaxial and abaxial petal surfaces, and pulling the tapes apart. The tape to which the adaxial epidermis was adhered was used for spectroscopic measurement.

4.5. Micromanipulation/vacuolar anthocyanins

Paradermal sections of the adaxial epidermis were taken from inner regions of fresh lisianthus petals, mounted on glass slides and viewed under an inverted microscope. Vacuolar contents were extracted from individual cells using glass micropipettes with a Narashige manual micromanipulator. The contents from 800 cell vacuoles were combined for one HPLC injection (analytical method as in Section 4.7) and flavonol and anthocyanin peaks were assigned on the basis of absorption spectra and retention times (see Section 4.8 for anthocyanin data). The ten flavonol glycoside peaks matched those obtained from an extract of inner petal (data not shown). Only three significant anthocyanin peaks were evident, and their retention times (22.8, 26.04 and 26.44 min) and on-line measured absorption spectra, matched those of compounds **1**, **4** and **5** (λ_{max}

277, 298 sh, 529; 278, 301, 312 sh, 527; 277, 298, 329, 529 nm) respectively.

4.6. Pigment extraction procedures

Fresh petal material was ground to a pulp and extracted with MeOH:H_2O:HOAc (11:5:1) for 1 h. Clear extract for analysis was prepared by centrifugation. Isolated AVIs were treated in the same way but the extracting solvent was MeOH:HOAc (1:1) or MeOH containing a few drops of 3 N HCl. Carnation petal macerates were extracted with MeOH:H_2O:3N HCl for anthocyanin:flavonol ratio determination.

4.7. Flavonoid analyses (Carnation)

Anthocyanin:flavonol ratios were determined by absorption spectroscopy of the clarified extracts. Anthocyanin levels were calculated from the absorption at 508 nm using an extinction coefficient of 36,000, and flavonols at 350 nm using an extinction coefficient of 15,000. HPLC analysis were carried out on extracts from blue-grey and pink petal regions using a Waters 600E solvent delivery system. Waters 996 diode array detector, and a Jasco 851-AS intelligent sampler, results being analyzed using Waters Millenium 2010 software. An injection volume of 20 μl was used with a Merck LiChrospher 100RP-18 endcapped column (5 μm, 4 × 119 mm). Elution (0.8 ml/min, 30°) was performed using a solvent system comprising solvent A (1.5% H_3PO_4) and solvent B (HOAc–CH_3CN–H_3PO_4–H_2O (20:24:1.5:54.5) mixed using a linear gradient starting with 80% A, decreasing to 33% A at 30 min, 10% A at 33 min, and 0% A at 39.3 min. Flavonols were detected at 352 nm and anthocyanins at 530 nm. Both petal types gave the same anthocyanin and flavonol profiles, with anthocyanin peaks at 12.54 (major) and 14.64 min, and flavonol peaks at 10.67, 19.06 (major), 20.0 (major) and 22.43 (major). On line spectra: (RT 12.54): λ_{max} 267.4, 329.0, 410 sh, 500.7 nm; (RT 14.64): λ_{max} 267.4, 331.4, 425.8, 503.1 nm; (RT 10.67): 267.4, 290 sh, 345.7 nm; (RT 19.06, 20.0, 22.43): 265.1, 300 sh, 348.1 nm.

4.8. Flavonoid analyses (Lisianthus)

HPLC analyses were carried out as described for carnations and the anthocyanin profiles are as presented in Fig. 3. Retention times (minutes) for anthocyanins are as follows: **1** (22.85), **2** (25.14), **3** (25.49), **4** (26.18), **5** (26.54), **6** (27.45), **7** (27.93), **8** (28.68), **9** (29.17). Relevant on-line spectra are detailed in the text. Electrospray–MS were determined at the MS unit, HortResearch, Palmerston North, NZ., on freeze-dried extracts of isolated AVIs and on a CC-purified sample of **2**, and recorded in both +Ve and −Ve ion modes. Relevant data are presented in the text. Semi-quantitative ICP–MS analyses were carried out at ESR, Gracefield, NZ on isolated AVI material (1 mg), and on wash solution and a total petal extract as "blanks". Of the 64 metals quantified only Aluminium (190, 120, 7400 ppb respectively), Iron (100, 100, 100 ppb), Rubidium (-, -, 100 ppb), Zinc (34, 150, 70 ppb), Calcium (1210, 1910, 1300 ppb) and Magnesium (44, 210, 1650 ppb) exceeded 100 ppb.

5. Two-dimensional isoelectric focusing analysis

AVIs isolated as described in Section 4.3 were treated with a solution of 10% TCA, 90% acetone and 0.07% 2-β-mercaptoethanol to liberate the majority of the anthocyanin and to precipitate protein. After a 45 min incubation at −20°C the precipitated material was collected by centrifugation (14,000 × *g* for 10 min at 4°C). The supernatant was removed and the pellet washed in acetone and subsequently dried under vacuum. The pellet was solubilised in a solution of 9.8 M urea, 2% Triton X-100, 100 mM Tris–Cl pH (8.8) and 100 mM dithiothreitol (DTT). After incubation at RT for 2 h any insoluble material was removed by centrifugation (14,000 × *g* for 15 min at RT). The solubilised proteins were fractionated using 2D electrophoresis. The isoelectric focusing for the first dimension was carried out using a pH 3–10 NL Immobiline DryStrip gel strip and DryStrip kit (Amersham Pharmacia Biotech, Auckland New Zealand) as per manufacturers instructions. The DryStrip was rehydrated overnight in a solution of 9.8 M Urea, 2% Triton X-100, 1% IPG-buffer (pH 3–10), 100 mM DTT and trace amounts of bromophenol blue. The protein sample was added directly to the reswelling solution and the strip rehydrated overnight at RT. The first dimension IEF separation was carried out using a Multiphor II Flatbed electropheresis unit (Amersham Pharmacia Biotech) for a total of 56 kVh. The strips were then removed and equilibrated once with equilibrium buffer (50 mM Tris–Cl pH (8.8), 6 M urea, 30% (v/v) glycerol, 2% (w/v) SDS and trace amounts of bromophenol blue) containing DTT and once with buffer containing iodoacetamide, according to manufacturers instructions. The second dimension SDS-PAGE was run on a 8–18% precast ExcelGel SDS gel (Amersham Pharmacia Biotech) using a Multiphor II flatbed electrophoresis unit, according to manufacturers instructions. The proteins were visualised by both Coomassie and silver staining using the PlusOne silver stain kit (Amersham Pharmacia Biotech) according to manufacturers instructions.

Acknowledgements

The authors are grateful to Dr. E Swinny of Industrial Research for access to the results of his lisianthus and

Sinningia studies; to Dr. K Ryan of Industrial Research for carrying out the electron microscopy, to Dr Connie Nozzolillo, Dept Biology, University of Ottawa, Canada for background and historical information; to Jasmina Stanojevic, School of Biological Sciences, University of Auckland, New Zealand for her painstaking isolation of the contents of hundreds of vacuoles; and to the Marsden Fund (NZ) for financial support via programme IRL701.

References

Asen, S., Griesbach, R.J., Norris, K.H., Leonhardt, B.A., 1986. Flavonoids from *Eustoma* grandiflorum flower petals. Phytochemistry 25, 2509–2513.

Asen, S., Stewart, R.N., Norris, K.H., 1975. Anthocyanin, flavonol copigments, and pH responsible for larkspur flower colour. Phytochemistry 14, 2677–2682.

Baranac, J.M., Petranovic, N.A., Dimitric-Markovic, J.M., 1996. Spectrophotometric study of anthocyan copigmentation reactions. 2. J. Agric. Food Chem. 44, 1333–1336.

Binding, H., Nehls, R., 1977. Regeneration of isolated protoplasts to plants in *Solanum dulcamara*. Z. Pflanzenphysiol. 85, 279–280.

Brouillard, R., Dangles, O., 1994. Flavonoids and flower colour. In: Harborne, J.B. (Ed.), The Flavonoids-Advances in Research Since 1986. Chapman and Hall, London, pp. 565–586.

Cormier, F., 1997. Food colourants from plant cell cultures. In: Johns, T., Romeo, J.T. (Eds.), Functionality of Food Phytochemicals — Recent advances in Phytochemistry, Vol. 31. Plenum Press, London and New York, pp. 201–218.

Cormier, F., Do, C.B., 1993. XXVII *Vitis vinifera* L. (grapevine): in vitro production of anthocyanins. In: Bajaj, Y.P.S. (Ed.), Biotechnology in Agriculture and Forestry, Vol. 24, Medicinal and Aromatic Plants, V. Springer Verlag, Berlin, pp. 373–386.

Deroles, S.C., Bradley, M.J., Schwinn, K.E., Markham, K.R., Bloor, S.J., Manson, D.G. et al., 1998. An antisense chalcone synthase cDNA leads to novel colour patterns in lisianthus (*Eustoma grandiflorum*) flowers. Molecular Breeding 4, 59–66.

Gamborg, O.L., Murashige, T., Thorpe, T.A., Vasil, I.K., 1976. Plant tissue culture media. In vitro 12, 473–478.

Gonnet, J.-F., Hieu, H., 1992. In situ microspectrophotometric and microspectrocolorimetric investigation of vacuolar pigments in flowers of carnation (*Dianthus caryophyllus*). J. of Horticultural Science 67, 663–676.

Harborne, J.B., 1967. Comparative Biochemistry of the Flavonoids. Academic Press, London (p. 18).

Harris, P.J., 1983. Cell walls. In: Hall, J.L., Moore, A.L. (Eds.), Isolation of Membrane and Organelles from Plant Cells. Academic Press, London, pp. 25–53.

Hemleben, V., 1981. Anthocyanin carrying structures in specific genotypes of *Matthiola incana* R.Br.. Z. Naturforsch 36c, 925–927.

Hoshino, T., Goto, T., 1990. Effects of pH and concentration on the self-association of malvin quinonoidal base — electronic and circular dichroic studies. Tetr. Letters 31, 1593–1596.

Kubo, H., Nozue, M., Kawasaki, K., Yasuda, H., 1995. Intravacuolar spherical bodies in *Polygonum cuspidatum*. Plant Cell Physiol. 36, 1453–1458.

Lin, M., Shi, Z., Francis, F.J., 1992. A simple method of analysis for *Tradescantia anthocyanins*. J. of Food Science 57, 766–767.

Linsmaier, E.M., Skoog, F., 1965. Organic growth factor requirements of tobacco tissue cultures. Physiol. Plant 18, 100–127.

Markham, K.R., 1996. Novel anthocyanins produced in petals of genetically transformed lisianthus. Phytochemistry 42, 1035–1038.

Markham, K.R., Ofman, D.J., 1993. Lisianthus flavonoid pigments and factors influencing their expression in flower colour. Phytochemistry 34, 679–685.

Mitchell, K.A., Markham, K.R., Boase, M.R., 1998. Pigment chemistry and colour of *Pelargonium* flowers. Phytochemistry 47, 355–361.

Morgan, E.R., 1998. Callus production from protoplasts of *Cyclamen persicum*. Plant Cell Tissue and Organ Culture 55, 63–65.

Murashige, T., Skoog, F., 1962. A revised medium for rapid growth and bioassays of tobacco tissue cultures. Physiol. Plant 15, 473–479.

Nozue, M., Kubo, H., Nishimura, M., Yasuda, H., 1995. Detection and characterisation of a vacuolar protein (VP24) in anthocyanin-producing cells of sweet potato in suspension culture. Plant Cell Physiol. 36, 883–889.

Nozue, M., Yamada, K., Nakamura, T., Kubo, H., Kondo, M., Nishimura, M., 1997. Expression of a vacuolar protein (VP24) in anthocyanin-producing cells of sweet potato in suspension culture. Plant Physiol. 115, 1065–1072.

Nozzolillo, C., 1994. Anthocyanoplasts: organelles or inclusions? Polyphenols Actualites, No. 11, pp. 16–18.

Nozzolillo, C., Ishikura, N., 1988. An investigation of the intracellular site of anthocyanoplasts using isolated protoplasts and vacuoles. Plant Cell Rep. 7, 389.

Nozzolillo, C., Anderson, J., Warwick, S., 1995. Anthocyanoplasts in the Brassicaceae: does their presence serve as a chemotaxonomic marker within the family? Polyphenols Actualites, No. 12, pp. 25–26.

Pecket, R.C., Small, C.J., 1980. Occurrence, location and development of anthocyanoplasts. Phytochemistry 19, 2571–2576.

Schwinn, K.E., Davies, K.M., Deroles, S.C., Markham, K.R., Miller, R.M., Bradley, M.J. et al., 1997. Expression of an *Antirrhinum majus* UDP-glucose: flavonoid-3-*O*-glucosyltransferase transgene alters flavonoid glycosylation and acylation in lisianthus (*Eustoma grandiflorum* Grise.). Plant Science 125, 53–61.

Small, C.J., Pecket, R.C., 1982. The ultrastructure of anthocyanoplasts in red-cabbage. Planta 154, 97–99.

Yasuda, H., 1974. Studies on "bluing effect" in the petals of red rose II. Observation on the development of the tannin body in the upper epidermal cells of bluing petals. Cytologia 39, 107–112.